DOI: 10.1021/ic1000792

Inorganic Chemistry
Article

Capturing Hydrolysis Products in the Solid State: Effects of pH on Uranyl Squarates under Ambient Conditions

Clare E. Rowland and Christopher L. Cahill*

Department of Chemistry, The George Washington University, 725 21st St. NW, Washington, D.C. 20052

Received January 14, 2010

Two uranyl squarates, $(UO_2)_6(C_4O_4)_3(OH)_6O_2 \cdot 9H_2O \cdot 4NH_4$ (**1**; a = 16.6897(7) Å, cubic, $I23$) and $(UO_2)(C_4O_4)(OH)_2 \cdot 2NH_4$ (**2**; a = 8.5151(4), b = 15.6822(8), c = 7.3974, orthorhombic, *Pbcm*), have been synthesized from ambient aqueous solutions as a function of pH. Oligomerization of the uranyl cation from monomeric pentagonal bipyramids (pH < 5) to $[(UO_2)_3O(OH)_3]$ trimers (5 < pH < 8) in **1** and ultimately $[(UO_2)(OH)_2]_n$ chains (7 < pH < 8) in **2** is observed. This evolution of speciation versus pH is consistent with what has been observed in solution and thus may be represented by the uranyl hydrolysis equilibrium, $mUO_2^{2+} + nH_2O \leftrightarrow [(UO_2)_m(OH)_n]^{2m-n} + nH^+$. Structural systematics, physical properties, and a discussion of species selectivity by squarate anions are presented.

Introduction

Hybrid materials consist of inorganic components joined by organic linkers and are being studied for applications as diverse as luminescence and gas storage.[1−4] The organic species from which these materials are assembled is, with some exceptions,[5] identical to the one that was intentionally introduced into the reaction. Hydrolysis of the metal may, on the other hand, result in a wide variety of inorganic building units. Uranium(VI) crystal chemistry, for instance, exhibits discrete building units ranging from monomers to hexamers as well as infinite chains and sheets.[1,6−9] Which of these building units is likely to emerge in the reaction product is often something of a mystery; and our poor understanding of the factors that favor one building unit over another remain one of the obstacles to predicting crystal structures from the starting materials.[10]

Hydrolysis of the uranyl cation (UO_2^{2+}) in solution has been studied extensively as a function of pH, temperature, ionic strength, etc (eq 1):[11]

$$mUO_2^{2+} + nH_2O \leftrightarrow [(UO_2)_m(OH)_n]^{2m-n} + nH^+ \qquad (1)$$

The hydrolysis equation suggests that at higher pH oligomerization of the uranyl cation is expected to occur in conjunction with hydrolysis; and indeed, previous studies have reported the evolution of oligomeric uranyl species below pH 4, with oligomers dominating the solution above pH 4.5.[11,12] The occurrence of oligomeric building units in the solid state follows logically from our understanding of oligomerization of the uranyl cation in solution. Exactly how hydrolysis prior to crystallization ultimately manifests itself in the solid state, however, is not entirely clear.

As hydrolysis is readily influenced by manipulating the pH of a solution, we have conducted a systematic study of the solid-state reaction products of the uranyl cation and a simple organic acid as a function of pH to elucidate the correlation between hydrolysis and building units. Crystal growth has been used with the intent of "freezing" the uranyl cation into its coordination environment, ideally by capturing building units from the solution. For this purpose, we have selected squaric acid (Scheme 1) for its versatile coordination modes and its demonstrated success in forming hybrid materials with f-elements.[13−16]

*Corresponding author. Telephone: (202) 994-6959. E-mail: cahill@gwu.edu.

(1) Cahill, C.; de Lill, D.; Frisch, M. *CrystEngComm* **2007**, *9*, 15–26.
(2) James, S. L. *Chem. Soc. Rev.* **2003**, *32*, 276–288.
(3) Rosi, N. L.; Eckert, J.; Eddaoudi, M.; Vodak, D. T.; Kirn, J.; O'Keeffe, M.; Yaghi, O. M. *Science* **2003**, *300*(5622), 1127.
(4) Allendorf, M. D.; Bauer, C. A.; Bhakta, R. K.; Houk, R. J. T. *Chem. Soc. Rev.* **2009**, *38*, 1330–1352.
(5) Zhang, X.-M. *Coord. Chem. Rev.* **2005**, *249*(11−12), 1201–1219.
(6) Leciejewicz, J.; Alcock, N. W.; Kemp, T. J. *Struct. Bonding* (*Berlin, Ger.*) **1995**, *82*, 43–84.
(7) Burns, P. C. *Can. Mineral.* **2005**, *43*(6), 1839–1894.
(8) Thuéry, P.; Nierlich, M.; Souley, B.; Asfari, Z.; Vicens, J. *Dalton Trans.* **1999**, 2589–2594.
(9) Duvieubourg, L.; Nowogrocki, G.; Abraham, F.; Grandjean, S. *J. Solid State Chem.* **2005**, *178*(11), 3437–3444.
(10) Deifel, N. P.; Cahill, C. L. *Cryst. Eng. Comm.* **2009**, *11*(12), 2739–2744.
(11) Grenthe, I.; Fuger, J.; Konings, R. J. M.; Lemire, R. J.; Muller, A. B.; Nguyen-Trung, C.; Wanner, H. *Chemical Thermodynamics of Uranium*, 2nd ed.; Nuclear Energy Agency, Organization for Economic Co-operation and Development: Issy-les-Moulineaux, France2004.
(12) Sylva, R. N.; Davidson, M. R. *Dalton Trans.* **1979**, 465–471.
(13) Hall, L. A.; Williams, D. J. *Adv. Inorg. Chem.* **2001**, *52*, 249–291.
(14) Wilson, A. S. *Cryst. Struct. Commun.* **1982**, *11*(3), 809–13.
(15) Petit, J.-F.; Gleizes, A.; Trombe, J.-C. *Inorg. Chim. Acta* **1990**, *167*(1), 51–68.
(16) Liu, Y.-S.; Ming-Feng, T.; Lii, K.-H. *Dalton Trans.* **2009**, 9781–9786.

Published on Web 03/11/2010

Table 1. Synthetic Conditions for **1** and **2**

	1	**2**
$UO_2(NO_3)_2 \cdot 6H_2O$ (g; mmol)	0.251; 0.50	0.249; 0.50
$C_4H_2O_4$ (g; mmol)	0.058; 0.51	0.114; 1.0
H_2O (g; mmol)	1.53; 85	1.51; 84
NH_4OH (μL; mmol)	300; 2.9	700; 6.7
pH_i	5.53	6.87
pH_f	5.24	5.15
temperature (°C)	ambient	90
time (days)	2	3
yield	76.9%	91.4%
elemental analysis	C 6.20, 6.20%	C 10.59, 10.63%
(observed, calculated)[a]	H 1.80, 1.73%	H 2.16, 2.23%
	N 2.43, 2.41%	N 6.19, 6.20%

[a] Via combustion, Galbraith Laboratories, Knoxville, Tennessee.

Scheme 1. Squaric Acid

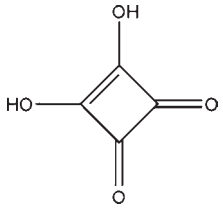

Herein, we report the synthesis and characterization of two novel uranyl squarates, including a three-dimensional framework $(UO_2)_6(C_4O_4)_3(OH)_6O_2 \cdot 9H_2O \cdot 4NH_4$ (**1**) and a one-dimensional coordination polymer $(UO_2)(C_4O_4)(OH)_2 \cdot 2NH_4$ (**2**). Additionally, we describe the trends in uranyl hydrolysis that are evident from the formation of compounds **1** and **2** as a function of pH. We further place these observations in the context of the only previously reported uranyl squarate, $(UO_2)(C_4O_4)(H_2O)$.[14]

Experimental Section

Synthesis. Caution! While the uranyl nitrate, $UO_2(NO_3)_2$, used in these experiments contained depleted uranium, standard precautions for handling radioactive material should be observed. All starting materials used in these synthetic reactions are available commercially and were used as obtained from the supplier.

Reactions of uranyl nitrate hexahydrate and squaric acid ($H_2C_4O_4$) were prepared in 1:1 molar ratios (0.50:0.50 mmol) in glass vials. To these were added 1.5 mL water (84 mmol) and incremental amounts of 9.6 N NH_4OH (0, 100, 200, 300, 400, and 500 μL NH_4OH). With the addition of 500 μL NH_4OH (pH 9.4) and above, a poorly crystalline product is observed. Based on identification of this product (PDF 14−0340),[17] it does not appear that the squaric acid incorporates into the crystalline phase, suggestive of a loss of crystallinity of uranyl squarates between 400 and 500 μL (pH 8.0 and 9.4). This point will be addressed in greater detail below.

The reaction vials were placed on the bench for two days, after which the mother liquor was decanted, and the remaining crystals were washed in water and sonicated in ethanol in preparation for subsequent characterization. Synthetic conditions under which we obtained **1** and **2** in highest yield are shown in Table 1, where **1** still contained a trace amount of **2**. Note that **2** was obtained in pure form only under hydrothermal conditions, in which reactants were sealed in a 23 mL Teflon lined Parr bomb and placed in an isothermal oven for three days. The bomb was then allowed to cool to room temperature over approximately 8 h, and the solid reaction products were treated similarly to reaction products formed under ambient conditions.

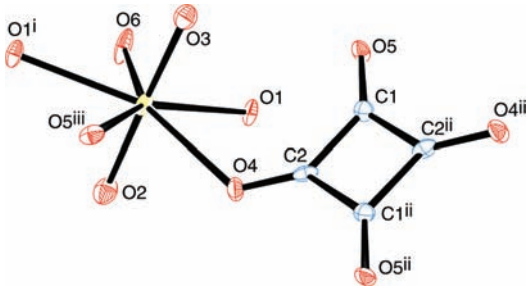

Figure 1. The local coordination geometry of **1**, represented with a 50% probability thermal ellipsoid plot. Symmetry transformations: i = z, x, y; ii = $-z + 1/2, -x + 1/2, y - 1/2$; and iii = y, z, x.

Table 2. Summary of Crystallographic and Structure Refinement Data from **1** and **2**

	1	**2**
empirical formula	$C_{12}H_{40}N_4O_{41}U_6$	$C_4H_8N_2O_8U$
FW	2324.62	450.114
temp (K)	100(2)	100(2)
λ (Mo Kα)	0.71073	0.71073
color	yellow	orange
habit	cube	plate
crystal system	cubic	orthorhombic
space group	*I*23	*Pbcm*
a (Å)	16.6897(7)	8.5151(4)
b (Å)	16.6897(7)	15.6822(8)
c (Å)	16.6897(7)	7.3974(4)
α (°)	90	90
β (°)	90	90
γ (°)	90	90
V (Å^3)	4648.9(3)	988.07(9)
Z	4	2
D_{calc} (g·cm^{-3})	2.978	3.026
μ (mm^{-1})	20.906	16.456
R_{int}	4.97%	6.13%
$R_1{}^a$ [$I > 2\sigma(I)$]	2.32%	1.91%
$wR_2{}^a$ [$I > 2\sigma(I)$]	7.80%	4.65%

[a] $R_1 = \sum||F_o| - |F_c||/\sum|F_o|$; $wR_2 = (\sum[w(F_o^2 - F_c^2)^2/\sum[w(F_o^2)^2])^{1/2}$

X-ray Structure Determination. Single crystals of both **1** and **2** were isolated from the bulk reaction products and mounted on a MicroMount needle (Mitegen). Reflections were collected from 0.5° φ and ω scans at 100 K on a Bruker SMART diffractometer with APEXII CCD detector and Mo Kα source. The APEX II software suite[18] was used to integrate the data and to apply an absorption correction.[19] Structures were solved using direct methods and refined with SHELX-97.[20] Publication materials were prepared using the WinGX software suite,[21] and figures were made with CrystalMaker.[22] Ambiguity in the position of hydrogen (H) atoms on ammonium cations prevented assignment. Any hydroxyl groups were identified using bond valence summation (Supporting Information, SI1).[23,24] H atoms on hydroxyl groups coordinated to U were not evident in the Fourier electron difference map and were, therefore, not

(17) *PDF-2, Powder Diffraction File*; International Centre for Diffraction Data: Newton Square, PA, **2005**.

(18) *APEXII Software Suite 2008.3−0*; Bruker AXS: Madison, WI, **2008**.
(19) Sheldrick, G. *SADABS, Siemens Area Detector ABSorption Correction Program*, 2008/1; University of Göttingen: Göttingen, Germany, **2008**.
(20) Sheldrick, G. *Acta Crystallogr.* **2008**, *A64*, 112–122.
(21) Farrugia, L. *J. Appl. Crystallogr.* **1999**, *32*, 837–838.
(22) Palmer, D. *CrystalMaker for Mac OS X*, 8.2.2; CrystalMaker Software Limited: Oxfordshire, England, 2009.
(23) Burns, P. C.; Ewing, R. C.; Hawthorne, F. C. *Can. Mineral.* **1997**, *35*, 1551–1570.
(24) Brese, N. E.; O'Keeffe, M. *Acta Crystallogr.* **1991**, *B47*, 192–197.

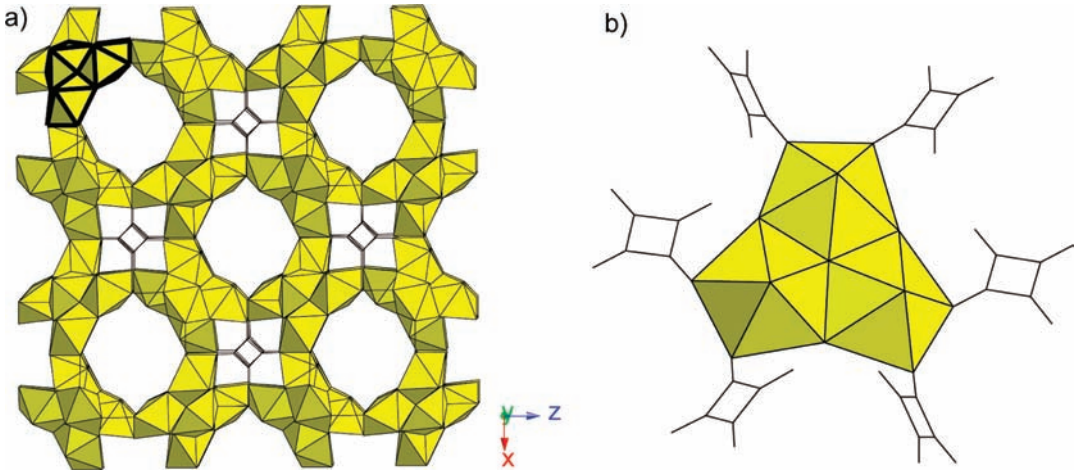

Figure 2. (a) Packing diagram of **1**, shown down [010], illustrates the channels that result from the coordination of uranyl trimers to squarate linkers. A trimer outlined in bold is shown in b. Disordered solvent water and NH_4^+ occupy the void volume but could not be crystallographically modeled and are absent from this representation. (b) Local view of the trimer and coordinated squarate anions.

assigned. Crystallographic data for **1** and **2** are summarized in Table 2.

A large accessible void volume in **1** required the use of Platon's SQUEEZE function[25] to assign residual electron density to disordered solvent. The resultant 1063 e^-/unit cell in a void space of 1823.3 $Å^3$ was accounted for with solvent water and ammonium, where the proportions were assigned based on the nitrogen reported in the elemental analysis. Assignment of 72 molecules of water and 32 molecules of ammonium, respectively, per unit cell accounts for this residual electron density and gives 9 H_2O and 4 NH_4^+ per formula unit. This allotment of electron density also to ammonium accounts for charge balance. Although the solvent was not accounted for in the structural model, it has been included in the formula entry of the CIF file, Supporting Information.

Structure solution and refinement of **2** proved interesting. The data were initially integrated in an orthorhombic cell and solved and refined in space group *Pbcm*. Positional disorder in the squarate anion across the mirror plane led to challenges assigning the two components of the disorder, which contributed to nonpositive definite thermal parameters for a number of atoms. The data were, therefore, integrated on a monoclinic cell, and the disorder was modeled in space group *Pc*. Successful refinement of this disorder showed that it would have been symmetrically distributed about the mirror plane in *Pbcm*, so a part −1 command was introduced in the orthorhombic space group to suppress the generation of bonds across the mirror plane. Problematic thermal parameters of two carbon atoms within the disordered segment of the structure required constraint to identical thermal parameters as carbons that were better behaved (EADP command), but doing so allowed all atoms to be refined anisotropicly without the appearance of atoms with nonpositive definite thermal parameters.

Powder X-ray diffraction data were collected on a Rigaku Miniflex diffractometer (Cu Kα, 3−60°) and analyzed with the Jade software package.[26] Calculated powder patterns were overlaid on observed patterns to identify phases present.

Characterization. In addition to X-ray diffraction, thermogravimetric analysis (TGA) and infrared spectroscopy (IR) were used to characterize **1** and **2**. TGA was performed on a Perkin-Elmer Pyris1 under nitrogen. The temperature ramp was 10 °C/min from 30 to 850 °C for **1** and from 30 to 700 °C for **2**. IR spectra were collected on a Perkin-Elmer Spectrum RXI FT-IR system. The samples were ground with spectroscopic grade KBr and pressed into a pellet. Eight scans were run from 400 to 4000 cm^{-1} with 4 cm^{-1} resolution. Neither **1** nor **2** exhibited fluorescence during a typical collection of an emission spectrum collected on a Shimadzu RF-5301 PC spectrofluorophotometer at an excitation wavelength of 365 nm and an emission wavelength of 400−800 nm with slit width 1.5 nm (excitation and emission) and a UV-35 filter. An excitation spectrum was also collected for both compounds (emission wavelength 500 nm, excitation wavelength 220−400 and 600−900 nm), and neither showed appreciable emission.

Results

Structure Descriptions. The crystal structure of **1** is defined by uranyl trimers assembled by squarate linkers into a three-dimensional framework. The uranyl cation (O2−U1−O3) is bound to five equatorial oxygen atoms (O1, $O1^i$, O4, $O5^{iii}$, O6; i = *z*, *x*, *y*; iii = *y*, *z*, *x*), as shown in Figure 1. O6 is a $\mu 3$ oxygen atom and is further coordinated to symmetry-generated $U1^i$ and $U1^{iii}$. O1 is a hydroxyl oxygen, as determined by bond valence summation[23,24] (Supporting Information, SI1); along with its symmetry equivalent $O1^i$, it binds U1 to $U1^i$ and $U1^{iii}$. The squarate anion is coordinated to U1 via O4 and to $U1^{ii}$ (ii = $-z + 1/2$, $-x + 1/2$, $y - 1/2$) via O5. The four-membered organic ring (C1, C2, $C1^{ii}$, $C2^{ii}$) sits on an inversion center. Coordination of the squarate to the uranyl trimers results in a three-dimensional framework with channels of maximum diameter 14.45 Å down [100], [010], and [001] as shown in Figure 2. Disordered solvent in the large accessible void space could not be modeled crystallographically and was instead handled using Platon's SQUEEZE function,[25] as described above. The ratio of H_2O to NH_4^+ was determined based on elemental analysis and was verified through charge balance. Important bond distances and angles, including torsion angles on the organic anion, are summarized in Table 3. Note that the U−U distance in this compound, 3.767 Å, is somewhat shorter than usual. The U−U distances in other structures that report uranyl trimers, in particular in those with a $\mu 3$ oxygen atom located at their center, range from 3.734[27] to 4.020 Å,[28] with an average of 3.851 Å.

(25) Spek, A. L. *J. Appl. Crystallogr.* **2003**, *36*, 7–13.
(26) *JADE*, 6.1; Materials Data, Inc: Livermore, CA, 2002.
(27) Vologzhanina, A. V.; Serezhkina, L. B.; Neklyudova, N. A.; Serezhkin, V. N. *Inorg. Chim. Acta* **2009**, *362*(14), 4921–4925.

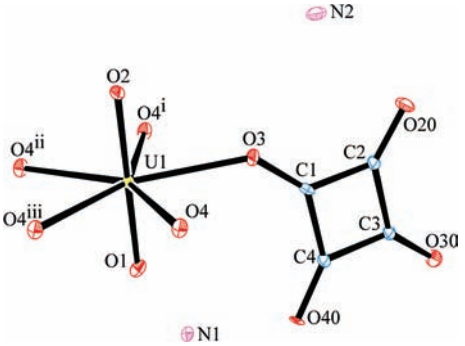

Figure 3. Thermal ellipsoid plot of **2** at the 50% probability level shows the local coordination environment of the uranyl cation. Symmetry transformations: i = $-x+1, -y+1, -z$; ii = $-x+1, -y+1, -z+1$; iii = $-x+1, -y+1, z-1/2$.

Table 3. Average Bond Distances (Å) and Angles (°)

	1	2
U=O	1.790(7)	1.794(4)
O=U=O	177.0(3)	180.0(2)
U−O	2.381(6)	2.364(5)
U−U	3.7674(5)	3.9027(2)
C−O	1.254(9)	1.258(10)
C−C	1.458(10)	1.462(12)
C−C−C	90.3(6)	91.1(6)
	89.7(6)	89.6(6)
		89.7(6)
		89.4(6)
O−C−C−O	1.9(2)	14.41(1.07)
	1.7(2)	13.75(1.78)
		13.34(1.58)
		11.42(2.19)

The crystal structure of $(UO_2)(C_4O_4)(OH)_2 \cdot 2NH_4$ (**2**) is defined by chains of edge-sharing pentagonal bipyramids with squarate anions that protrude into the interlayer. The asymmetric unit consists of a single U(VI) pentagonal bipyramid with a monodentate squarate anion coordinated to it. Five oxygen atoms occupy the equatorial plane of the uranyl cation (O1−U1−O2), two of which are crystallographically unique (O3, O4). The other three are generated through symmetry ($O4^i$, $O4^{ii}$, $O4^{iii}$; i = $-x+1, -y+1, -z$; ii = $-x+1, -y+1, -z+1$; iii = $-x+1, -y+1, z-1/2$). The squarate anion is bound to the uranyl cation through O3 and consists of C1, C2, C3, C4, O20, O30, and O40. The local coordination geometry of the structure is shown in Figure 3. Polymerization of the uranyl cation occurs by edge sharing through O4, a hydroxyl oxygen, as determined by bond valence summation (Supporting Information, SI1), and its symmetry equivalents, resulting in chains that propagate down [001] (Figure 4a). Squarate anions on adjacent chains experience $\pi-\pi$ interactions, with an intermolecular distance of 3.701 Å from center to center (Figure 4b). Two molecules of ammonium (N1 and N2) occur per asymmetric unit. Disorder in the squarate anion and in N1 about the mirror plane has been treated as described above. Important bond distances, angles, and torsion angles for **2** are summarized in Table 3.

(28) Delaigue, X.; Gutsche, C. D.; Harrowfield, J. M.; Ogden, M. I.; Skelton, B. W.; Stewart, D. F.; White, A. H. *J. Supramol. Chem.* **2004**, *16*(8), 603–609.

Powder X-ray Diffraction (PXRD). PXRD was vital in determining the evolution of phases as a function of pH. As shown in Figure 5, we observe the known Wilson structure, $(UO_2)(C_4O_4)(H_2O)$, under very acidic conditions. This phase remains the only one detectable by PXRD through pH = 4.7, after which the peaks associated with it diminish rapidly. The last traces of these peaks have disappeared by pH = 8.0. At pH = 5.5, we observe the first occurrence of **1**, which can be identified by its strongest peaks at 10.5° and 19.75° 2θ. These peaks can be tracked all the way through pH = 8.0. Peaks associated with **2** begin growing in at pH = 7.2. The most visible of these is the (110) reflection at 11.8° 2θ. Although this is not the largest of the calculated peaks, others, like that of the (100) peak at 10.3° 2θ, may be obscured by overlap with the (200) peak of **1** at 10.5° 2θ. Moreover, because crystals of **1** adopt a plate habit, preferred orientation may account for the relatively strong signal from this reflection as compared to others. At pH = 9.4, the reaction products are poorly crystalline. Aside from a peak at 16.5° 2θ, the observed pattern corresponds to an ammonia uranium oxide hydrate (PDF 14−0340), the observed and calculated patterns of which have been shown in Supporting Information, SI2.

PXRD patterns were also used to confirm the purity of the samples that were used to perform other characterization tests. The powder pattern of **1** (Supporting Information, SI3), shows a very minor impurity at 11.8° 2θ, which corresponds to the strongest observed reflection from **2**. The powder pattern from a hydrothermal preparation of **2** (Supporting Information, SI4) shows no impurities within the detection limits of the instrumentation.

Thermogravimetric Analysis. Thermogravimetric analysis (TGA) of **1,** shown in Supporting Information, SI5, resulted in three discrete weight loss steps. An initial weight loss of 7% corresponds to the loss of solvent water (calculated total weight loss 7.0%). The second weight loss of 12.5% (19.5% total) corresponds roughly to the loss of the squaric acid (calculated total weight loss 21.4%). The final weight loss of 9% corresponds to the loss of ammonium and hydroxyl groups and of bound oxygen as water. The total weight loss observed was 28.5%, which corresponds with a uranium oxide as the final product (calculated total weight loss 27.4%). PXRD confirms this (PDF 31−1416; Supporting Information, SI6).

TGA of **2**, plotted in Supporting Information, SI7, produced a 34.0% weight change, which corresponds to the loss of both squaric acid and ammonium ions from the structure (calculated weight loss 32.8%).

Infrared Spectroscopy. Both **1** and **2** exhibit comparable IR spectra (Supporting Information, SI8 and SI9). A broad peak centered around 3750 cm^{-1} can be attributed to the O−H stretch of bound hydroxyl groups and, in the case of **1**, to solvent water. Sharper peaks in this region result from the N−H stretch of ammonium. Uranyl stretching is observed around 910 and 750 cm^{-1} (asymmetric and symmetric, respectively) in **1** and around 870 and 760 cm^{-1} (asymmetric and symmetric, respectively) in **2**. The carbonyl stretch occurs for both compounds around 1500 cm^{-1}.

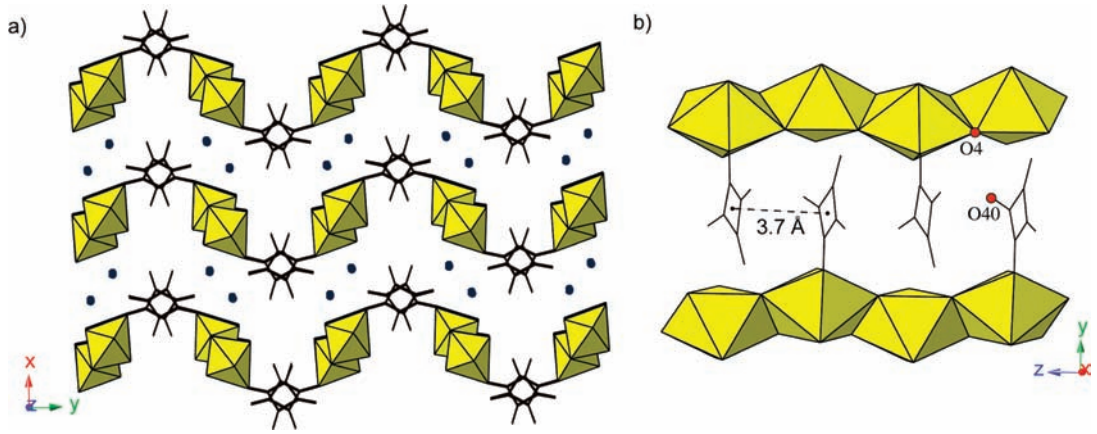

Figure 4. (a) Edge-sharing pentagonal bipyramids form chains with squarate anions that hang into the interlayer. Green spheres represent ammonium ions. Chains propagate in the [001] direction. (b) A view down [100] of **2** shows $\pi-\pi$ interactions between squarate anions on neighboring chains.

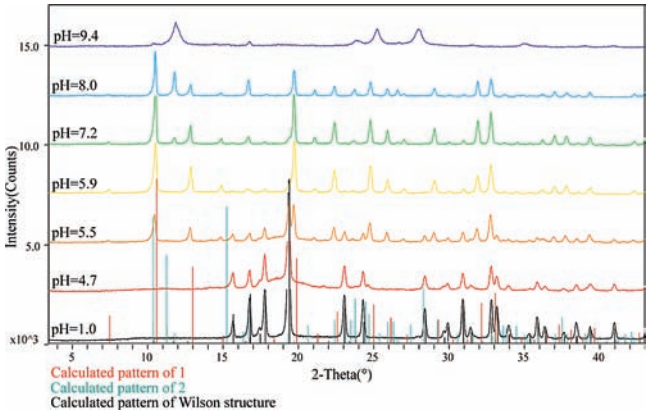

Figure 5. PXRD pattern of room temperature synthesis at 1:1 metal: ligand ratio. As pH increases, peaks attributed to **1** and **2** grow in and peaks from the Wilson structure disappear.

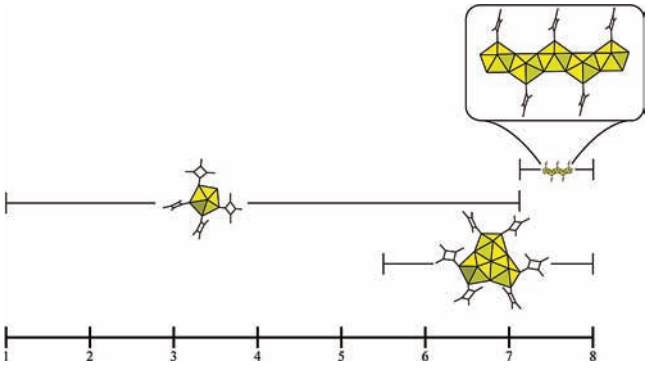

Figure 6. The uranyl building unit and coordinated organic ligand are shown here as a function of the initial pH of the solution from which crystals were grown. The Wilson structure occurs under very acidic conditions. At higher pH, **1** begins to form concurrently with the Wilson structure. At neutral pH and above, **1** and **2** both appear, while the Wilson structure is no longer observed.

Discussion

Hydrolysis of the uranyl cation in solution has been well studied under ambient conditions and is known to result in uranyl oligomerization.[11] The effects of this oligomerization can be seen in the solid state as growth of the uranyl building unit from monomer to polymer. To extrapolate from solution–phase studies to the solid state, we would expect to observe a monomeric uranyl building unit in crystals grown under highly acidic conditions. With increase in solution pH and, therefore, in hydrolysis, we might expect to observe polymerized uranyl building units in the crystal structure.

This anticipated observation holds true for this study. As illustrated in Figure 6, the monomeric Wilson structure[14] is observed at low pH. As pH increases to 5.5, we observe the evolution of **1**, which is composed of a uranyl trimer building unit. Thus, with increased hydrolysis, we see the expected oligomerization in solution reflected in the solid-state reaction product. At still higher pH, **2** is observed, although under these reaction conditions it remains a minor phase. This species nonetheless demonstrates the anticipated further polymerization to a chain. Moreover, under hydrothermal conditions we expect the hydrolysis equilibrium to lie further to the right (eq 1). The fact that we observe **2** in pure form only under hydrothermal conditions is further suggestive that it is indeed hydrolysis in the solution that is pushing the formation of polymerized building units in the solid state.

Although a wide variety of uranyl species may exist in solution simultaneously, especially between pH 4–6,[11] we observe a maximum of two building units at a time in our solid-state products. This is perhaps due to a preference of the ligand for certain building units to which it binds selectively in solution. In this case, as the preferred building units are removed from solution during crystallization, we would expect the hydrolysis equilibrium to be re-established and effectively replenish the supply of the preferred species.

It is interesting to note that although trimers account for a significant fraction of uranyl species in solution over a substantial pH range, dominating the aqueous phase over most of the range from pH < 4.5 to pH > 10 at concentrations of 1 mM,[11] they have been observed with relative infrequency in hybrid materials.[27–32] The formation of this trimeric species in the solid state has been attributed to the $(UO_2)_3(OH)_5^+$ complex that has been identified as the predominant species in solutions ranging from pH < 4.5 to approximately pH $= 7$ at roughly 1 mM concentrations.[11] The

(29) Back, D. F.; Oliveira, G. M. d.; Lang, E. S. *Z. Anorg. Allg. Chem.* **2007**, *633*(5–6), 729–733.
(30) Gatto, C. C.; Lang, E. S.; Kupfer, A.; Hagenbach, A.; Abram, U. *Z. Anorg. Allg. Chem.* **2004**, *630*(8–9), 1286–1295.
(31) Lintvedt, R. L.; Heeg, M. J.; Ahmad, N.; Glick, M. D. *Inorg. Chem.* **1982**, *21*(6), 2350–2356.
(32) Szabo, Z.; Furo, I.; Csoregh, I. *J. Am. Chem. Soc.* **2005**, *127*(43), 15236–15247.

loss of a water molecule from this complex would result in the formation of the trimer seen in the crystalline reaction product, namely $(UO_2)_3O(OH)_3^+$. We observe this trimer in the solid state from pH 5.5−8. Although this range differs slightly from the range over which we expect to observe the trimeric complex in solution, it should be noted that the pH was measured immediately following the addition of reagents to the reaction vessel and not at the time of crystal formation. Unfortunately, the pH of synthesis was documented in only two previous occurrences of the trimer in the solid state. One of these, pH ∼ 6,[29] is consistent with the pH range over which we observe the trimer. The other occurs at a more basic level, pH > 10,[32] and corresponds to the synthetic region where our reaction products are largely amorphous and fail to incorporate the squarate anion.

In addition to the greater degree of polymerization of the uranyl cation in **2**, we also observe noteworthy torsion in the squarate anion. The greatest torsion angle that we report is 14.41(1.07)°, and the slightest is 11.42(2.19)°. By contrast, the torsion angles measured in **1**, 1.7(2)° and 1.9(2)°, are quite small. The appearance of torsion in the squarate anion is not unheard of, however, and, although a search of the Cambridge Structural Database shows that most squarates fall within 5° of being flat, outliers appear at nearly 50° (results in Supporting Information, SI10).[33]

Significant distortion of the carbon ring, resulting in a buckling of the squarate anion and considerable torsion angles, has been observed previously in several lanthanide squarates.[15] As in **2**, these distorted lanthanide squarates experience $\pi-\pi$ interactions. The authors, however, propose that the lanthanide cations, lying outside the plane of the squarate anion, exert perpendicular forces that distort the carbon ring. The uranium metal centers in **2** lie in the plane of the squarate, so this hypothesis seems unable to account for our observation of torsion. More likely, we can attribute both the disorder and the torsion in the structure to hydrogen-bonding interactions between squarates protruding into the interlayer and to hydroxyl groups that bridge uranyl centers on adjacent chains. The distance from a hydoxyl group to the nearest squarate oxygen (O4−O40) is approximately 2.7 Å. This interaction could conceivably pull the squarate oxygen atom (O40), and with it the entire squarate anion, toward the hydroxyl groups on either side of the uranyl center, taking the anion slightly out of the plane of the uranium (refer to Figure 4b). The fact that these squarate anions are monodentate, unlike the bi- and tridentate anions in the lanthanide squarates, would give the squarate anion more freedom to "lean" out of the uranyl plane, which would also account for the disorder about the mirror plane.

(33) Allen, F. H. *Acta Crystallogr.* **2002**, *B58*, 380–389.

Conclusion

The effects of pH and, by extension, hydrolysis of the uranyl cation on the reaction products of uranyl nitrate and squaric acid have been investigated here. Two new uranyl squarates have been described, one containing a uranyl trimer building unit and one in which the uranyl cation polymerizes into chains. The growth of the uranyl building unit from a monomer at low pH to a trimer and then to a chain at higher pH suggests that oligomerization that occurs in solution as a function of pH manifests itself in turn in the solid state. An investigation of the influence of hydrothermal conditions on the uranyl squarate system will follow.

Acknowledgment. This material is based upon work supported as part of the Materials Science of Actinides, an Energy Frontier Research Center funded by the U.S. Department of Energy, Office of Science, Office of Basic Energy Sciences under Award Number DE-SC0001089. Additional support was from the Chemical Sciences, Geosciences, and Biosciences Division, Office of Basic Energy Sciences, Office of Science, Heavy Elements Program, U.S. Department of Energy, under Grant DE-FG02-05ER15736 at George Washington University. X-ray diffraction equipment was purchased with National Science Foundation funding (DMR-0348982 and -0419754).

Supporting Information Available: Bond valence summation values, powder X-ray diffraction patterns, TGA plots, and IR spectra are available for compounds **1** and **2**. Also available are a plot of torsion angles in squarates from the CSD. This material is available free of charge via the Internet at http://pubs.acs.org. CIFs may also be obtained free of charge from The Cambridge Crystallographic Data Centre via www.ccdc.cam.ac.uk/data_request/cif by referencing CCDC 761715 and 761716.